Journal of Statistical Physics, Vol. 55, Nos. 1/2, 1989

Explicit Construction of Steady State of a Model of Chemical Turbulence

C. Yeung[1,2]

Received November 24, 1987; revision received December 1, 1988

Using only the microscopic dynamics, the nonequilibrium steady state of a one-dimensional cellular automaton (CA) model of chemical turbulence is explicitly constructed. A coding is found which decomposes the CA into three interacting shift systems, each of which has an independent steady-state distribution. It was previously shown that the steady state of this model is a Gibbs state. Hence the steady state can be represented in the form $Z^{-1}e^{-F}$, where F is the "conditional energy" of the system such that all conditional probabilities are continuous. It is shown that the conditional energy of this model has an approximate expression in terms of familiar models from equilibrium statistical mechanics.

KEY WORDS: Steady state; Gibbs state; chemical turbulence.

1. INTRODUCTION

In equilibrium statistical mechanics the steady state (or invariant measure) can be obtained by minimizing the appropriate thermodynamic potential, but no general procedure is known for obtaining the steady state of a far-from-equilibrium system. At this level in our understanding, it is useful to study simple but nontrivial models of nonequilibrium systems. In particular, it is natural to study cellular automata (CA), since the mathematics of equilibrium system is best defined for lattice models with finite cell states.[1-3] In this paper, we study the steady state of a one-dimensional CA with irreversible dynamics. The CA was introduced by Oono and Kohmoto

[1] Department of Physics and Materials Research Laboratory, University of Illinois at Urbana-Champaign, Urbana, Illinois 61801.

[2] Present address: Department of Physics and Astronomy, University of Pittsburgh, Pittsburgh, Pennsylvania 15232.

0022-4715/89/0400-0357$06.00/0

to model chemical turbulence.[4] The steady state is explicitly constructed from the microscopic dynamics and an approximate form for the energy of the steady state is found.

Equilibrium states are Gibbs states. This means, roughly speaking, that the equilibrium state is the thermodynamic limit of finite-set probability measures of the form $Z^{-1}e^{-F}$, where F is the conditional energy, and the finite-set conditional probabilities are continuous and positive. A formal mathematical definition is given in Appendix A, but the fact that equilibrium states are Gibbs states has more than formal consequences. For example, a Gibbs measure ensures the existence of the thermodynamic limit of the expectation value of any continuous intensive observable, without which there is no guarantee that performing computer simulations on larger and larger lattices will give the correct expectation value.

For nonequilibrium systems, there is no general argument that the steady state is a Gibbs state, but it is known that the steady states of particular systems are Gibbs states. Takahashi showed that the steady states of all 1D reversible CA are Gibbs distributions[5] and Oono and Yeung showed that the steady state of the 1D CA studied in this paper is also a Gibbs distribution.[6]

This paper is organized as follows: In Section 2 the chemical turbulence model is described. The dynamics does not obey detailed balance, as the individual cells have a stable (discrete) limit cycle which is perturbed by interactions with other cells. In Section 3 we describe the coding which decomposes the CA into three shift systems. In Section 4 we demonstrate that the steady-state probability of any sequence of cells can be calculated in principle and hence the steady state can be found. In addition, we calculate the steady-state probabilities of some specific $0M1$ sequences. In Section 5 we find an approximate form for the conditional energy which generates the steady state. Section 6 is a summary of the results.

2. THE MODEL

The CA model studied in this paper was originally introduced by Oono and Kohmoto[4] to study chemical turbulence[7] as can be exhibited by the Belousov–Zhabotinskii reaction (see, e.g., ref. 8). In this paper, we are not concerned with the physical process, so we ignore the physical motivation for the model. For a complete description of this model, see Oono and Kohmoto[4] and Oono and Yeung.[6]

Time, space, and the cell state space are all discrete in a CA (see, e.g., refs. 9 and 10). The chemical turbulence model is a 1D three-state nearest-neighbor CA; individual cells in the CA can have states 0, 1, or M ($M \geqslant 1$) and the state of a cell after an update depends only on the states of the cell

and its two nearest-neigbor cells before the update. The CA is completely defined by the update rules for the triplets; we call these the local update rules. The local update rules are given by

$$a_{i,t+1} = T_l(x_{i,t}) = \begin{cases} M & \text{if } 0.5 \geqslant x_{i,t} \\ 1 & \text{if } 0.5 < x_{i,t} \leqslant 1.5 \\ 0 & \text{if } x_{i,t} > 1.5 \end{cases} \tag{2.1}$$

where $i \in Z$ (the set of all integers) and $a_{i,t} \in \mathscr{A} \equiv \{0, 1, M\}$ is the state of cell i at time t. Here $x_{i,t}$ is a weighted average of three cells,

$$x_{i,t} = \alpha a_{i,t} + (1-\alpha)(a_{i-1,t} + a_{i+1,t})/2 \tag{2.2}$$

where $\alpha \in [0, 1]$. The CA is basically a system of diffusively coupled discrete limit cycles; there is no quiescent state; in the absence of interactions among the cells (i.e., $\alpha = 1$), each individual cell has a stable three-cycle (for $M > 1.5$). Each cell will undergo the discrete cycle with 0 followed by M followed by 1 and then back to 0. In ref. 4 this model is called the $0M1$ model.

The phase diagram for the $0M1$ model is shown in Fig. 1; the control parameters are M and α. The dashed lines are boundaries between different CAs (i.e., as M and α are varied so that a dashed line is crossed, the update

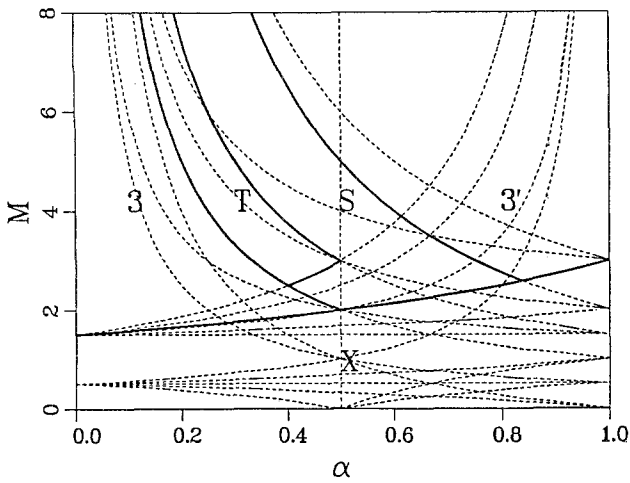

Fig. 1. The phase diagram for the $0M1$ model.[6] The dashed lines are boundaries of areas with the same local rules. The solid lines indicate different macroscopic phases. The symbols T and S indicate the "turbulent" phase and "soliton" phases respectively. The T_1 subphase is the area around $\alpha = 1/3$ and $M = 4$. The other symbols indicate other phases not discussed in the text.

rules for one or more of the triplets are changed). The spatial-temporal patterns are the observable, so we group together different CAs with similiar spatial temporal patterns into "macroscopic phases." As shown in Fig. 2, there are two types of interesting spatial-temporal patterns. The patterns are obviously different; the first pattern seems to contain solitons while the second seems to be turbulent. Therefore, we call the phases the S phase (for soliton) and the T phase (for turbulent). The regions in parameter space with these phases are delimited by solid lines in Fig. 1. In this paper we will be interested in the T phase. Table I shows the local update rules for one of the CAs (the regime around $\alpha = 0.3$, $M = 4$) in the T phase. This particular CA is denoted the T_1 subphase.

3. THE CODING

The fundamental idea of the coding is to decompose the CA into three shift systems. The distributions of the shift systems are asymptotically independent, so the steady state can be found by obtaining the distributions on the three subsystems separately. The decomposition is done in two steps. First, the system is mapped into a soliton picture which, in ref. 6, is called the P-I representation. The dynamics in the P-I representation looks like

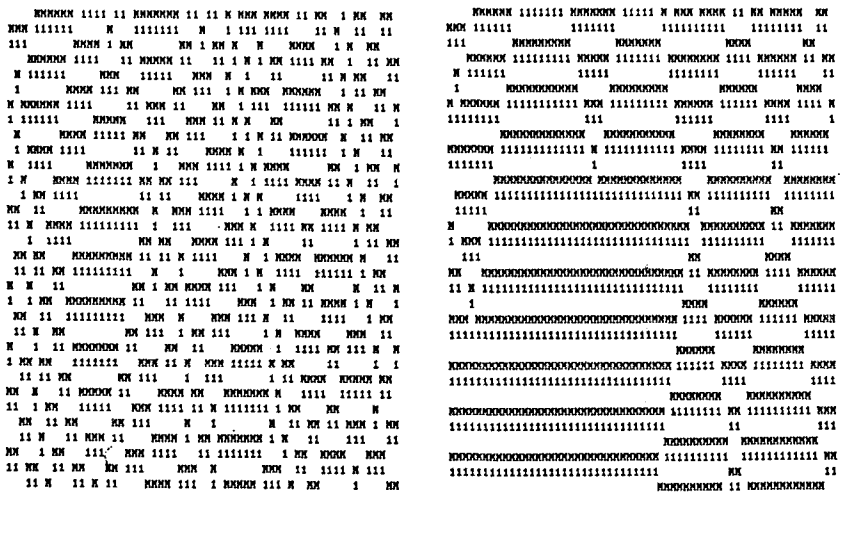

T S

Fig. 2. Typical space-time patterns of the $0M1$ model.[4] Time flows from top to bottom. The horizontal direction is the spatial direction. The empty cells actually contain 0. The T phase looks turbulent.

Table I. The Local Update Rules for the T_1 Subphase[a]

000	001	$00M$	101	$10M$	$M0M$
⇓	⇓	⇓	⇓	⇓	⇓
M	M	0	M	0	0
010	001	$01M$	111	$11M$	$M1M$
⇓	⇓	⇓	⇓	⇓	⇓
0	0	0	0	0	1
$0M0$	$0M1$	$0MM$	$1M1$	$1MM$	MMM
⇓	⇓	⇓	⇓	⇓	⇓
1	1	1	1	1	1

[a] Only 18 rules are shown, since the others can be obtained by the symmetry of the update rules. The triplets with adjacent M and 1 are not present in the steady state. The rules for the remaining triplets are the same for all CA in the T phase.

that of a 1D hard rod gas. Second, a variation of a map introduced by Sinai[11] is used to decompose the "hard rod gas" into three interacting shift systems. This is called the P-II representation. Explicit proofs are given in ref. 6; in most cases the proofs are simple and are made by inspection of the local update rules in the T phase.

We start with the $0M1$ system with initial measure μ_0 on configuration space $\Omega_0 \equiv \{0, 1, M\}^Z$ and, for simplicity, we choose μ_0 to be the uniform product measure which assigns probability 1/3 to each state. We notice that if the initial state is updated twice, all configurations with 1's and M's adjacent to one another are eliminated. The local rules for the remaining triplets (i.e., those without adjacent M and 1) are the same for all subphases within the T phase. This accounts for the similarity of the spatial-temporal patterns in the T phase; the dynamics of all CAs in the T phase are the same after two updates. The system obtained after two updates is denoted $(T, \Omega_1, \mu_1) \equiv (T, T^2\Omega_0, \mu_0 T^{-2})$, where T is the CA update. Note that any differences in the steady states of the CAs in the T phase are due to differences in μ_1. In general, the differences between the steady states of the subphases are difficult to observe.

The first coding is the map to the P-I representation. We denote the P-I representation by (S_1, Σ_1, ν_1) and the one-to-one map to P-I by Φ: $(T, \Omega_1, \mu_1) \to (S_1, \Sigma_1, \nu_1)$. The idea behind this mapping is that instead of considering the state of each cell, we can define the CA by the types and

dynamics of the points where the states of the cells change. We call such a point a domain wall or, for simplicity, just a wall.

The first step is to classify and find the dynamics of all isolated domain walls. Consider a section of the lattice of the form $MMM011$. After one update the section becomes 111000, after two updates, $000MMM$, and after three updates, $MM0111$; the original form is recovered but shifted one site to the left, so a left-traveling soliton consists of three types of walls. There is an analogous set of walls for the right-going soliton. These are all the possible types of walls in Ω_1, for a total of six types of walls.

We can consider these isolated walls as solitons with an internal phase ϕ of period three; we set $\phi = 0$ for $MMM011$, $\phi = 1$ for 111000, and $\phi = 2$ for $000MMM$. After this, ϕ is again 0, but the soliton is shifted to the left. We can eliminate the internal phase variable by mapping to a larger lattice, so the isolated soliton shifts one site at every update. This map Φ is shown in Table II and an example of coding is shown in Fig. 3. Each soliton is assigned a position and direction on the larger lattice based on the position, internal phase, and direction of the soliton on the original lattice.

The dynamics in the P-I representation is simple. A noninteracting soliton will simply shift one site in its direction. The only interaction occurs when two solitons traveling in opposite directions are either one or four sites apart; in that case both solitons reverse directions. An example of the dynamics is shown in Fig. 4. The dynamics is similiar to that of a hard-rod gas. We use a coding devised by Sinai[11] to separate left- and right-going solitons. This coding was originally used by Sinai[11] and Aizenman *et al.*[12] to show that a 1D hard rod gas in Bernoulli.

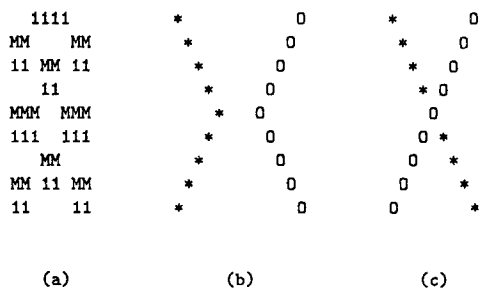

Fig. 3. (a) An example of two walls interacting; the format is the same as in Fig. 2. (b) The configuration in part (a) mapped into the P-I representation. Stars and circles indicate the positions of the two solitons. The interaction looks like an elastic hard-rod collision. (c) The situation in part (b) if the interaction distance of four sites is subtracted between the two solitons and the symbols are exchanged during a collison. The solitons seem to pass through one another.

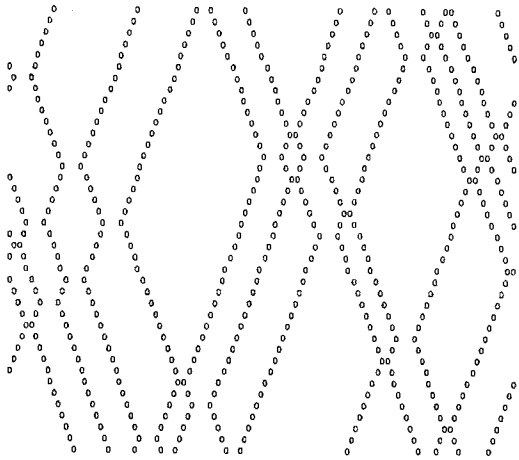

Fig. 4. An example of the dynamics in the P-I representation. This figure shows the $0M1$ model on a 40-site lattice after mapping to the P-I representation. Note that this looks like a set of solitons with variable-distance hard-core interactions.

The basic idea of Sinai's coding is that collisions only occur when solitons are a specific distance apart; so if this distance between solitons is eliminated, the solitons will seem to pass through one another (see Fig. 3c). The distance subtracted depends on whether neighboring solitons are an even or an odd number of sites apart. We keep track of the distance subtracted between a pair of solitons by assigning a spin $+1$ or -1 to each soliton.[3] Solitons have the same spin if the pair are an even number of sites apart and whether two solitons are an even or an odd number of sites apart is unchanged by the dynamics. The one-to-one map Θ from the P-I representation to the new, P-II representation is given by

$$\begin{aligned} x_0 &= y_0 \\ x_i &= x_{i-1} + (y_i - y_{i-1}) - q(y_i - y_{i-1}) \qquad \text{if} \quad i > 0 \\ x_i &= x_{i+1} - (y_{i+1} - y_i) + q(y_{i+1} - y_i) \qquad \text{if} \quad i < 0 \end{aligned} \tag{3.1}$$

where

$$q(y) = \begin{cases} 4 & \text{if } y \text{ is even} \\ 1 & \text{if } y \text{ is odd} \end{cases} \tag{3.2}$$

[3] In ref. 6, a color, red or blue, was assigned to each soliton instead of spin. Spin is used here in order to use more standard terminology.

and y_i is the P-I position of the $i+1$ soliton at, or to the right of, the origin and x_i is the soliton's P-II position. The spin of a soliton is defined by whether y_i is even or odd at some arbitrarily chosen time t_0,

$$s_i = \begin{cases} +1 & \text{if } y_i(t_0) \text{ is even} \\ -1 & \text{if } y_i(t_0) \text{ is odd} \end{cases} \tag{3.3}$$

The direction of the solitons is unchanged by Θ,

$$\text{dir}_i = \begin{cases} +1 & \text{if solution } i \text{ is going to the right} \\ -1 & \text{if soliton } i \text{ is going to the left} \end{cases} \tag{3.4}$$

We denote the P-II representation by (S_2, Σ_2, v_2).

In the P-II representation, the CA update shifts all solitons one step in the solitons' direction. If a collision occurs, the indices, spins, and directions of the colliding solitons are all exchanged. There is an added complication, however, because the first soliton with $y \geqslant 0$ serves as a reference point for the map from P-I to P-II. If a soliton passes through $y = 0$, the reference point is changed. In order to maintain the uniqueness of the map from P-I to P-II, it is necessary to change the indices and positions accordingly. Let

$$z_i' = x_i(t) + \text{dir}_i(t) \tag{3.5}$$

The exchanges at collisions are accounted for by

$$z_i = \begin{cases} z_{i+1}' & \text{if } z_i' > z_{i+1}' \\ z_{i-1}' & \text{if } z_i' < z_{i-1}' \\ z_i' & \text{otherwise} \end{cases} \tag{3.6}$$

where z_i is the new position of the ith soliton if the reference point does not change. Let $\varepsilon = 1$ if $z_0 < 0$, $\varepsilon = -1$ if $z_{-1} \geqslant q(z_0 - z_{-1})$, and $\varepsilon = 0$ otherwise. Here q is the function defined in (3.2). The entire update in the P-II representation is

$$\begin{aligned} x_i(t+1) &= z_{i+\varepsilon} + \varepsilon q(z_\varepsilon - z_0) \\ s_i(t+1) &= s_{i+\varepsilon}(t) \\ \text{dir}_i(t+1) &= \text{dir}_{i+\varepsilon}(t) \end{aligned} \tag{3.7}$$

If the index 0 soliton passes the origin to the right, the index 1 soliton becomes the new reference soliton ($\varepsilon = +1$); then all indices are decremented by 1 and all positions incremented by $q(z_1 - z_0)$. If the index -1 soliton

Table II. Direction and Phases of a Soliton between Sites n and $n+1$ in the $\{0, 1, M\}$ Representation and the Corresponding Soliton Position in the P-I Representation[6],[c]

Configuration	Phase	Direction	Position in P-I
$1\underline{0}M$	0	Right	$3n$
$\check{M}\underline{0}1$	1	Right	$3n+1$
$\underline{M}0\check{1}$	2	Right	$3n+2$
$\underline{M}01$	0	Left	$3n+2$
$1\underline{0}\check{M}$	1	Left	$3n+1$
$\check{1}\underline{0}M$	2	Left	$3n$

[a] Site n is underlined.

becomes the new reference soliton ($\varepsilon = -1$), then all indices are incremented by 1 and all positions decremented by $q(z_0 - z_{-1})$.

The P-II representation can be considered to be three interacting shift systems: all left-going soliltons as one subsystem L, all right-going solitons as another subsystem R, and the spin sequence as a third subsystem S. The three systems interact when solitons pass the origin, causing all three systems to be shifted by an appropriate amount. The dynamics of the three subsystems are shown in Fig. 5.

Finally, to close this section, we note some restrictions on the positions of solitons. The separation between a soliton and the next soliton

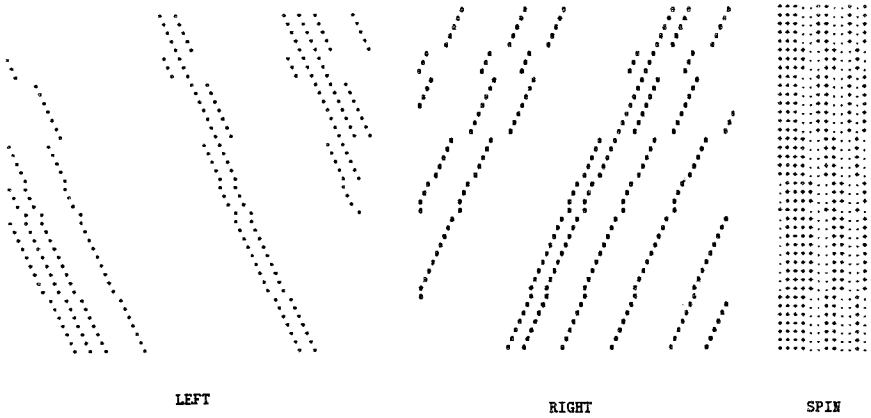

Fig. 5. The example in Fig. 2 mapped into the P-II representation. The system can now be divided into three parts; a left-going lattice (left), a right-going lattice (middle), and a spin lattice (right). Here we have used + (+1 spin) and · (−1 spin).

going in the same direction is $4+6i$ $(i=0, 1, 2,...)$ and the separation between a soliton and the next soliton going in the opposite direction is $2i$ $(i=0, 1, 2,...)$. The positions of the solitons are all odd or all even at any one time. These restrictions can be verified by following the coding.

4. THE STEADY STATE

The main point of Section 3 is that the $0M1$ model can be decomposed into three interacting shift systems. In this section we will show that the distributions of the three shift systems are asymptotically independent of one another, so that steady state can be found by calculating the distribution on each subsystem separately. We show how the distributions can be obtained and then, in Section 5, use the result to find an approximate form for the energy.

Let the initial uncorrelated configuration be at $t=0$. The maximum range of correlations, after two updates $(t=2)$, is five sites. This configuration can be mapped into the P-II representation, so sections of the P-II subsystems which are close together will be correlated. These correlated sections, however, are separated by the dynamics.

The displacement of each subsystem is the sum of a systematic shift plus an extra shift due to solitons passing the origin. The extra shift is proportional to the difference between the number of solitons passing the origin to the left and the number passing to the right. By considering the symmetries of the CA rules and of the initial distribution (i.e., both the local rules and the initial distribution are invariant under space inversion and space translation), the distributions of left- and right-going solitons must be the same and be translationally invariant. Therefore, the number of left- and right-going solitons passing the origin during t updates are both of $O(t)$ for large t and the net shift due to solitons passing the origin must be of $O(\sqrt{t})$. The result is that the displacement of right-going solitons during t updates is $t+O(\sqrt{t})$, the displacement of left-going solitons is $-t+O(\sqrt{t})$, and the displacement of the spin sequence is of $O(\sqrt{t})$. Initially, regions close to each other on the L, R, and S subsystems are correlated with each other, but as t becomes large, these initially correlated regions rapidly separate from one another. Therefore, for large t, there is no correlation between the separate subsystems; correlations only exist within each individual subsystem. The steady state is then the product measure of the distributions of the three subsystems. The distribution on each subsystem is unchanged by the shift dynamics; so we can find the steady state by finding the distribution of each subsystem at any update t at which the map into the P-II representation is possible.

We will obtain the steady state for the T_1 subphase. In this subphase,

there are no adjacent 1's and M's after one update, so we can use the P-II coding at $t=1$. This makes the calculation easier, since the maximum range of correlations at $t=1$ is only three sites; however, the discussion below can be easily adapted for the other subphases in the T phase. We denote the steady state by $(T, \Omega_1, \mu_\infty)$. The steady state can be obtained in three steps:

1. The probability distribution μ_1 on Ω_1 after one update is calculated at $t=1$. This distribution can be found in a systematic manner by using conditional probabilities.
2. The distribution of spins is calculated. The spins of two neighboring solitons are parallel if, in the P-I representation, the solitons are an even number of sites apart, and the spins are antiparallel if the solitons are an odd number of sites apart.
3. The distributions of left- and right-going solitons are obtained. The distribution of the left-going and right-going solitons are the same, so the calculation is only necessary for one of the subsystems.

Let $P_m(a_1 a_2 \cdots a_m)$ be the probability w.r.t. μ_1 of the m-length sequence $a_1 a_2 \cdots a_{m-1} a_m$, and $P_m(a \mid a_1 a_2 \cdots a_m)$ be the conditional probability of state $a \in \mathscr{A}$ if the states of the m cells immediately to the right are $a_1 a_2 \cdots a_m$. As shown in Appendix B, if the sequence $a_1 a_2 \cdots a_{m-1}$ contains any of the subsequences M, 00, 01, 10, or $1 \cdots 10$, the conditional probabilities are independent of a_m,

$$P_m(a_0 \mid a_1 a_2 \cdots a_{m-1} a_m) = P_{m-1}(a_0 \mid a_1 a_2 \cdots a_{m-1}) \tag{4.1}$$

Therefore, the μ_1 probability of any finite-length $0M1$ sequence can be obtained from the probability of length 2 sequences and the conditional probabilities $P_1(a \mid M)$, $P_2(a \mid 0M)$, $P_2(a \mid 00)$, $P_2(a \mid 01)$, $P_2(a \mid 10)$, and $P_m(a \mid 11 \cdots 110)$ (for $\forall a \in \mathscr{A}$ and $m = 3, 4, 5, \ldots$). The $P_m(\bullet)$'s and $P_m(a \mid \bullet)$'s needed to calculate the μ_1 probability of any $0M1$ sequence are obtained in Appendix B and the values are shown in Table III.

The next step is to calculate the distribution on each of the three subsystems in the P-II coding. First, the distribution of spins is found. The point to remember is that two neighboring solitons have parallel (antiparallel) spins if, in the P-I representation, the solitons are an even (odd) number of sites apart. In order to calculate the probability of a n-length spin sequence, we need to sum over the μ_1 probabilities of all finite $0M1$ sequences, which, in the P-II coding, has n solitons and the correct spin sequence.

As a demonstration, we perform the calculation for two spin sequen-

Table III. The $0M1$ Probabilities Needed to Calculate the μ_1 Probabilities of Long $0M1$ Sequences[a]

$P_2(00)$	16/81	$P_2(11)$	15/81
$P_2(01)$	15/81	$P_1(MM)$	4/81
$P_2(0M)$	8/81		
$P_2(0\|00)$	1/3	$P_2(0\|0M)$	1/3
$P_2(1\|00)$	1/2	$P_2(1\|0M)$	1/2
$P_2(M\|00)$	1/6	$P_2(M\|0M)$	1/6
$P_2(0\|01)$	8/15	$P_1(0\|M)$	2/3
$P_2(1\|01)$	3/15	$P_1(1\|M)$	0
$P_2(M\|01)$	4/15	$P_1(M\|M)$	1/3
$P_3(010)$	25/243	$P_7(01^50)$	0.00635065
$P_4(0100)$	25/729	$P_8(01^60)$	0.00338702
$P_5(01^30)$	50/2167	$P_9(01^70)$	0.00183463
$P_6(01^40)$	25/2167	$P_{10}(01^80)$	0.00098788

[a] We need (a) the probabilities of length-2 $0M1$ sequences, (b) the conditional probabilities given M, 00, 01, and $0M$, and (c) the probabilities of m-length sequences beginning and ending with 0 with all 1's in between. The probabilities $P_m(01^{m-2}0)$ (here 01^k0 indicates there are k 1's between the two 0's) are shown up to $m = 10$.

ces. The distribution is symmetric w.r.t. flipping all spins, so it is only necessary to obtain the probability that the two spins are parallel and the probability the two spins are antiparallel. To calculate the probability that the spins are antiparallel, we must sum over all two-soliton sequences in which the two solitons, in the P-I representation, are an odd number of sites apart,

$$\begin{aligned} P_s(+-) = {} & P_3(0M0) + P_5(0MMM0) + P_7(0MMMMM0) + \cdots \\ & + P_3(010) + P_5(01110) + P_7(0111110) + \cdots \\ & + P_4(100M) + P_6(10000M) + P_8(1000000M) + \cdots \\ & + P_4(M001) + P_6(M00001) + P_8(M0000001) + \cdots \\ & + P_3(101) + P_5(10001) + P_7(1000001) + \cdots \\ & + P_3(M0M) + P_5(M000M) + P_7(M00000M) + \cdots \\ = {} & P_s'(-+) \end{aligned} \tag{4.2}$$

where all probabilities on the rhs are w.r.t. μ_1. The probability that the spins are parallel is given by the sum over all $0M1$ sequences with two

solitons, which, in the P-I representation, are an even number of sites apart,

$$\begin{aligned} P_s(++) = {} & P_4(0MM0) + P_6(0MMMM0) + \cdots \\ & + P_4(0110) + P_6(011110) + P_8(01111110) + \cdots \\ & + P_5(1000M) + P_7(10000M) + P_9(1000000M) + \cdots \\ & + P_5(M0001) + P_7(M00001) + P_9(M0000001) + \cdots \\ & + P_4(1001) + P_6(100001) + P_8(10000001) + \cdots \\ & + P_4(M00M) + P_6(M0000M) + P_8(M000000M) + \cdots \\ = {} & P'_s(--) \end{aligned} \tag{4.3}$$

The expressions can be evaluated using Table III. The result is $P_s(++)/P_s(+-) = 15/7$ {to obtain the actual probabilities, we divide P_s by $2 \times [P_s(++) + P_s(+-)]$}. The probability of longer spin sequences is calculated in the same manner as the two-spin sequences. The calculation can be made systematically, i.e., a simple computer program can be written. Table IV shows the probability of all sequences of five or less spins.

Using this result, we can find the relative probabilities of some two-soliton sequences. For example, the sequences $M0M$ and $M00M$ differ, in the P-II representation, only in that the spins of the two solitons are antiparallel in $M0M$ but are parallel in $M00M$. Therefore, in the steady state,

$$P_3(M0M)_\infty / P_4(M00M)_\infty = P_s(++)/P_s(+-) = 15/7 \approx 2.14$$

[here $P_m(\bullet)_\infty$ is the probability w.r.t. μ_∞]. This result is exact, but, as a check, a numerical simulation of the $0M1$ model on a 330-site lattice gives $P_3(M0M)_\infty / P_4(M00M)_\infty = 2.16 \pm 0.04$. Note that w.r.t. μ_1, $P_3(M0M)/P_4(M00M) = 3$.

As another example, the three-soliton sequences $M0M01$ and $M00MM01$ differ, in the P-II representation, only in that, in $M0M01$ the second soliton has a different spin from the others, while in $M00MM01$, all three solitons have the same spin. Therefore in the steady state, the ratio

$$P_5(M0M01)_\infty / P_7(M00MM01)_\infty = P_s(+-+)/P_s(+++) = 4.61$$

(Table IV), while w.r.t. μ_1, $P_5(M0M01)/P_7(M00MM01) = 9$.

We next obtain the distributions of right-going solitons. The soliton distribution is translationally invariant, so it is defined by the distribution of the separations between solitons. This distribution is calculated in the

Table IV. The Probability of Spin Sequences of Five or Fewer Spins[a]

(a) 5-spin probabilities			
+ − + − +	0.21650071	+ − + − −	0.10089543
+ − + + −	0.10038570	+ − + + +	0.04513681
+ − − + −	0.10038570	+ − − + +	0.05147652
+ − − − +	0.04495603	+ − − − −	0.02208127
+ + − + −	0.10089543	+ + − + +	0.04462708
+ + − − +	0.05147642	+ + − − −	0.02190049
+ + + − +	0.04513681	+ + + − −	0.02190049
+ + + + −	0.02298127	+ + + + +	0.01016373
(b) 4-spin probabilities			
+ − + −	0.31739614	+ − + +	0.14552251
+ − − +	0.15186222	+ − − −	0.06703730
+ + − +	0.14552251	+ + − −	0.07337701
+ + + −	0.06703730	+ + + +	0.03224500
(c) 3-spin probabilities			
+ − +	0.46291865	+ − −	0.21889952
+ + −	0.21889952	+ + +	0.09928230
(d) 2-spin probabilities			
+ −	0.68181817	+ +	0.31818181

[a] The probabilities are symmetric w.r.t. flipping all spins, so only sequences beginning with + spin is shown.

same manner as the spin distribution. As noted in Section 3, neighboring solitons going in the same direction must be $4 + 6i$ sites apart ($i = 0, 1, 2, \ldots$).

As a demonstration, we consider the probability that two right-going solitons are four sites apart; this is the sum over all $0M1$ sequences consisting of two right-going solitons four sites apart with any number of left-going solitons between them. There are six sequences consisting of just the two solitons: $M|00|1$, $M|000|1$, $\check{M}|010|M$, $\check{M}|0110|M$, $10|M|0\check{1}$, and $10|MM|0\check{1}$, where $\check{x}$ means not x and the position of a soliton is indicated by |. There are another eight sequences consisting of two right-going solitons four sites apart with one left-going soliton between them: $M|0|M0|\check{1}$, $M|00|M0|\check{1}$, $M|0|MM0|\check{1}$, and $M|00|MMM0|\check{1}$, and $\check{M}01|1|0|1$, $\check{M}0|11|0|1$, $\check{M}0|1|00|1$, and $\check{M}0|11|00|1$. The probability that two neighboring right-going solitons are four sites apart is the sum of the μ_1 probabilities over the 14 $0M1$ sequences,

$$
\begin{aligned}
P_{\text{sep}}(4) = {} & P_4(M001) + P_5(M0001) + P_5(\check{M}010M) \\
& + P_6(\check{M}0110M) + P_5(10M0\check{1}) + P_6(10MM0\check{1}) \\
& + P_5(M0M0\check{1}) + P_6(M00M0\check{1}) + P_6(M0MM0\check{1}) \\
& + P_7(M00MM0\check{1}) + P_5(\check{M}0101) + P_6(\check{M}01101) \\
& + P_6(\check{M}01001) + P_7(\check{M}011001)
\end{aligned}
$$

To find the probability that the solitons are ten sites apart, we need to sum the μ_1 probabilities of $42\,0M1$ sequences. There are even more terms for larger separations. Nevertheless, the probabilities can be calculated systematically. Table V shows the two-soliton separation probabilities for $i \leqslant 9$. The probability drops off exponentially for $i \geqslant 6$.

To find the steady-state probability for general $0M1$ sequences, we must find the separation probabilities for sequences with more than two solitons going in one direction. The probabilities for such larger sequences can also be found systematically. For example, we have found the four-soliton separation probabilities $P_{\text{sep}}(i, j, k)$ for all $i, j, k \leqslant 40$, where $P_{\text{sep}}(i, j, k)$ is the probability that, in the P-II coding, the first soliton is i sites away from the second, the second is j sites from the third, and the third is k sites from the fourth. These probabilities will be used to find an approximate form for the free energy of the soliton subsystems.

Table V. The Probability That Nearest Neighbor Solitons Are Separated by $4+6i$, $P_{\text{sep}}(4+6i)$, and the Corresponding Nearest Neighbor Interaction Energy $f(4+6i)$[a]

i	$P_{\text{sep}}(4+6i)$	$P(i-1)/P(i)$	$f_1(4+6n)$
0	0.543209910	—	0.61026
1	0.255488992	0.470332	1.36458
2	0.113627821	0.444746	2.17487
3	0.049497757	0.435613	3.00583
4	0.021549616	0.435365	3.83740
5	0.009385843	0.435563	4.66855
6	0.004088129	0.435560	5.49967
7	0.001780627	0.435560	6.33078
8	0.000775569	0.435560	7.16191
9	0.000775569	0.435560	7.99303

[a] For large i, $P_{\text{sep}}(4+6i) = \frac{1}{8}(1+\sqrt{5})\,P_{\text{sep}}(4+6(i-1))$ and $f(4+6i) = f(4+6(i-1)) + 0.831$. Here $f(4)$ is chosen so that $\sum_i e^{-f(4+6i)} = 1$.

As with the spin distribution, we can use the separation probabilities to find the steady-state probabilities of some $0M1$ sequences. For example, in the P-II coding, $M001$ and $M00001$ differ in that the two right-going solitons are four sites apart in $M001$ but ten sites apart in $M00001$. The probability that there are no left-going solitons on the $4+6i$ sites is then sum over all configurations without left-going solitons on those sites; $\sum_{j\geqslant i+1}\sum_{k\geqslant j}P_{\text{sep}}(4+6k)$. To compute this sum, we use Table V and for $k\geqslant 9$, we use the asymptotic form $P_{\text{sep}}(4+6k)=0.43556\,P_{\text{sep}}[4+6(k-1)]$:

$$\frac{P_6(M00001)_\infty}{P_4(M001)_\infty}$$

$$= \frac{P_{\text{sep}}(10)}{P_{\text{sep}}(4)} \frac{\text{prob. of no left soliton on 10 sites}}{\text{prob. of no left soliton on 4 sites}}$$

$$= 0.4703 \times 0.4407 = 0.2071 \tag{4.5}$$

As a check, the simulation gives $P_6(M00001)_\infty/P_4(M001)_\infty = 0.211 \pm 0.05$.

5. THE ENERGY FUNCTIONAL

Oono and Yeung[6] have shown that the steady state of the T phase is a Gibbs random field; the steady state is the limit of finite set probabilities of the form $Z^{-1}e^{-F}$, where Z is the partition function and F is the conditional energy (see Appendix A). In this section we show that from the steady-state distribution we can find an approximate form for F, in the P-II representation, based on the Hamiltonians of some familiar equilibrium systems. In order to find the energy of a configuration in the $0M1$ representation one would then use the one-to-one P-II coding to map the configuration into the P-II representation.

The steady state is the product measure of three independent distributions. This means that the energy F is the sum of the energy for each subsystem,

$$F = F_S + F_L + F_R \tag{5.1}$$

where F_S is the energy of the spin configuration, F_L is the energy of the left-going solitions, and F_R is the energy of the right-going solitons.

The most general form for F_S is an Ising Hamiltonian with long-range and many-body interactions,

$$F_S = \sum_{i,n_1>0} J^{(2)}_{n_1} s_i s_{i+n_1} + \sum_i \sum_{n_3>n_2>n_1>0} J^{(4)}_{n_1,n_2,n_3} s_i s_{i+n_1} s_{i+n_2} s_{i+n_3} + \cdots \tag{5.2}$$

The terms involving an odd number of spins is zero since F is invariant with respect to a global flip of the spins. The spin coupling can be obtained from the spin distribution. First, assume that only the nearest neighbor coupling $J_1^{(2)}$ is nonzero. Then $J_1^{(2)}$ can be found from the two-spin distribution

$$\begin{aligned} J_1^{(2)} &= \tfrac{1}{4} \ln[P_s(+-)\, P_s(-+)/P_s(++)\, P_s(--)] \\ &= \tfrac{1}{2} \ln P_s(+-)/P_s(++) = 0.381 \end{aligned} \tag{5.3}$$

where the numerical result is found using Table IV. To check the consistency of the nearest neighbor approximation, we next assume that the interactions involve at most three adjacent sites, i.e., only the nearest neighbor coupling $J_1^{(2)}$ and the next nearest neighbor coupling $J_2^{(2)}$ are nonzero. If the nearest neighbor approximation is reasonable, $J_1^{(2)}$ obtained with this assumption must be close to (5.3) and $J_2^{(2)}$ must be small compared to $J_1^{(2)}$. We now need the three-spin distribution to obtain the couplings

$$J_1^{(2)} = \tfrac{1}{4} \ln P_s(+-+)/P_s(+++) = 0.385 \tag{5.4}$$

and

$$J_2^{(2)} = \tfrac{1}{4} \ln[(P(+--)\, P(++-)/P(+-+)\, P(+++)] = 0.0104 \tag{5.5}$$

Therefore the approximation (5.3) for $J_1^{(2)}$ seems to be reasonable. As a further check we can assume that interactions involve at most four adjacent sites. With this assumption, in addition to the two-body couplings $J_1^{(2)}$, $J_2^{(2)}$, and $J_3^{(2)}$, it is also possible that the four-body coupling $J_{1,2,3}^{(4)}$ is nonzero. These couplings are found from the four spin distributions. The four-body coupling is

$$\begin{aligned} J_{1,2,3}^{(4)} = \tfrac{1}{8}\{&\ln[P_s(+++-)\, P_s(++-+)\, P_s(+-++)\, P_s(+---)] \\ &- \ln[P_s(++++)\, P_s(++--)\, P_s(+-+-)\, P_s(+--+)]\} \\ = &-0.022 \end{aligned} \tag{5.6}$$

and

$$\begin{aligned} J_3^{(2)} = \tfrac{1}{8}\{&\ln[P_s(+++-)\, P_s(++--)\, P_s(+-+-)\, P_s(+---)] \\ &- \ln[P_s(++++)\, P_s(++-+)\, P_s(+-++)\, P_s(+--+)]\} \\ = &\, 0.0015 \end{aligned} \tag{5.7}$$

Using the four spin probabilities, we find $J_2^{(2)} = 0.0106$ and $J_1^{(2)} = 0.380$. This is again close to the results for $J_1^{(2)} = 0.381$ and $J_2^{(2)} = 0.0104$ given by

(5.3) and (5.5). We can find interaction with longer range, but allowing for the possibility of longer range interactions does not seem ao appreciably affect the values of the shorter range couplings. Furthermore, $J_3^{(2)}$ is one order smaller than $J_2^{(2)}$, and $J_{1,2,3}^{(4)}$ and is two orders smaller than $J_1^{(2)}$; so the longer range coupling is expected to be smaller still. Therefore, the nearest neighbor interaction seems to be the most significant term in F_S.

The distributions of left- and right-going solitons are translationally invariant, so the energy functional is a function only of the separation between solitons. The most general form of F_R is

$$F_R = \sum_i f(x_{i+1} - x_i) + \sum_{i, j_1, j_2} g_{j_1, j_2}(x_{i+j_1} - x_i, x_{i+j_2} - x_{i+j_1}) + \cdots \quad (5.8)$$

where x_i is the position of the ith right-going soliton. F_L is obviously of the same form. First assume that the only nonzero term is the two-body nearest neighbor interaction f. Then f can be found from the two-soliton separation distribution, $f \propto -\ln P_{\text{sep}}$. Table IV shows the values of f assuming only nearest neighbor interaction, and f_4 has been chosen so that $\sum_{i \geq 0} e^{-f(4+6i)} = 1$. We find that $f(4) = 0.610$, $f(10) = 0.136$, and f increases linearly for large i as $f(4+6i) = f(4+6(i-1)) + 0.831$. To check the consistency of the nearest neighbor approximation, we next assume that only the terms involving at most three adjacent solitons, f and $g_{1,1}$, are nonzero. Since f can always be absorbed into $g_{1,1}$, to fix the two-body term, we set $g_{1,1}(k_1, k_2)$ to 0 if either k_1 or $k_2 = 4$. Then f can be found from the four-soliton distribution;

$$f(4+6i) = -\ln\left[P_{\text{sep}}(4, 4+6i, 4) \Big/ \sum_{j=0}^{\infty} P_{\text{sep}}(4, 4+6j, 4) \right] \quad (5.9)$$

where P_{sep} is calculated using the method described in Section 4. Using (5.9), we find that $f(4) = 0.614$, $f(10) = 1.36$, and asymptotically $f(4+6i) = f(4+6(i-1)) + 0.831$. The values for f are close to the values found with the nearest neighbor assumption.

Since $g_{1,1}(4, 4+6i)$ is set to zero, the three-body interaction is given by

$$e^{-g_{1,1}(4+6i, 4+6j)} = e^{-2f(4)+f(4+6i)+f(4+6j)} \frac{P_{\text{sep}}(4, 4+6i, 4+6j, 4)}{P_{\text{sep}}(4, 4, 4, 4)} \quad (5.10)$$

For example, $g_{1,1}(10, 10) = 0.037$, $g_{1,1}(16, 10) = 0.035$, and $g_{1,1}(16, 16) = 0.029$. Since $f_{10} - f_4$ is ~ 0.75, the contribution from the two-body term is 20 times larger then the three-body contribution.

Our results indicate that the actual energy can be well approximated by including only nearest neighbor coupling terms, F_S by a nearest neighbor Ising model with antiferromagnetic coupling $\beta J = 0.38$ and F_L and F_R as a particle system with an interaction f (Table V) depending only on the separation between nearest neighbor particles.

As a demonstration, we use the approximate energy to calculate the probability of some $0M1$ sequences. The method used is the same as described in Section 4; map to the P-II representation and find the probability of each subsystem separately, except that, instead of using the steady state probability, we use $Z^{-1}e^{-F}$, where F is the approximate energy. We consider the sequences

(a) $10MM0M01001 \to 3R^- 7R^- 7L^+ 11L^- 15L^+ 17R^+$

(b) $M0110M00101 \to 2L^+ 8R^+ 12R^- 16R^+ 18L^- 20R^+$

(c) $10MM00M \to 3R^- 7R^- 7L^-$

(d) $M0M \to 2R^+ 2L^-$

The rhs is the P-II coding, where, for example, $5L^-$ indicates a spin -1 left-going soliton at site 5. To eliminate the Z^{-1} factor, the probabilities are calculated w.r.t. $P_3(M0M)_\infty$. Using the approximate energy,

$$
\begin{aligned}
P_3(M0M)_\infty &= Z^{-1}e^J\alpha \\
P_{12}(10MM0M01001)_\infty &= Z^{-1}(1-e^{-f(4)})\,e^{-[f(4)+f(10)]}e^{-2f(4)}e^J\alpha^5 \\
&= 0.000880P_3(M0M)_\infty \qquad (5.11) \\
P_{11}(M0110M00101)_\infty &= Z^{-1}(1-e^{-f(4)})e^{-[2f(4)+f(10)]}e^{-f(10)}e^{3J}\alpha^5 \\
&= 0.00887P_3(M0M)_\infty \\
P_7(10MM00M)_\infty &= Z^{-1}(1-e^{-f(4)})e^{-f(4)}e^{-2J}\alpha^2 \\
&= 0.0368P_3(M0M)_\infty
\end{aligned}
$$

where $\alpha = 1/(e^J + e^{-J})$. The actual steady-state probabilities, obtained used the method described in Section 4, are, for sequence (b), $0.000882P_3(M0M)_\infty$; for sequence (c), $0.000884P_3(M0M)_\infty$; and for sequence (d), $0.03613P_3(M0M)_\infty$. For the sequences considered, the probabilities (5.11) using the approximate energy are within 1% of the actual steady-state probabilities.

6. SUMMARY

We have calculated the steady state of a 1D CA model of chemical turbulence. The calculation is possible since the CA can be decomposed into

three interacting shift systems: a spin system and left- and right-going soliton systems. Initially, there are correlations among and within the three shift systems; however, the dynamics destroys the correlations among the shift systems while preserving the distribution within the individual subsystems. The calculation of the steady state is thus reduced to finding the distribution on the individual subsystems. This can be done in a straightforward manner. Interestingly, the initial state has no correlations beyond finite distances, but the elimination of correlations among the subsystems is accomplished by producing exponentially decaying correlations within each subsystem.

The steady state is a Gibbs field, so there must be an energy functional which generates the steady state. Since the steady-state distributions of the three subsystems are independent, the energy functional is the sum of the energies for the subsystems. We have found an approximate form for the energy functional based on the Hamiltonians of familiar equilibrium systems. The spin distribution is well approximated by the distribution of an Ising model with antiferromagnetic nearest neighbor coupling. For the soliton systems, we used an energy dependent only on the separation between neighboring solitons. If the system is closed (i.e., finite), the shift dynamics obviously conserves the energy.

In ref. 6 we showed that the T-phase dynamics in K (for Kolmogorov), which means that the Kolmogorov–Sinai entropy is positive (see, e.g., ref. 13).[4] This is reflected in the fact the correlations among the subsystems are all destroyed by the dynamics. This is actually a fairly common feature of many nonequilibrium systems studied so far; the dynamics makes the system uncorrelated in some sense. For example, van Beijeren and Schulman[14] (also see ref. 15) studied the fast rate limit of a lattice gas driven by an external electric field E; in this case the dynamics in the direction parallel to the E field are so fast that correlations in that direction can be ignored. In another case, an Ising system with two types of dynamics [spin flip (Glauber) and spin exchange (Kawasaki) dynamics] occurring at different temperatures was studied.[16,17] In this case the solution is found in the limit that the Kawasaki dynamics occurs at infinite temperature and at such a fast rate that the spins are uncorrelated on short length scales. This may account for why many nonequilibrium steady states so far studied show mean field behavior.

On a more technical level, one can extend the domain wall approach to other CAs: find all the domain walls present in the steady state and then characterize their dynamics. In higher dimensions the dynamics may be

[4] Even though the T-phase dynamics is K, it is strongly suspected that the dynamics is not Bernoulli, i.e., there is no one-to-one map.

very complicated, but for a 1D nearest neighbor CA the dynamics should be simple. The dynamics of the domain walls consists of translation, creation, destruction, and collision. So the complete classification of the types of domain walls and their dynamics would allow one to examine CA from a different and sometimes simpler viewpoint.

APPENDIX A

In this Appendix, we give the definition of a Gibbs state. Let Z^ν be a ν-dimensional lattice, $\mathscr{A}$ be the (finite) set of single cell states, and $\Omega \subseteq \mathscr{A}^{Z^\nu}$ be the set of all configurations on Z^ν. Let $\mathscr{F}$ be the family of all finite subsets of Z^ν and $\Omega_F \subseteq \mathscr{A}^F$ be the configuration space on $F \in \mathscr{F}$. Let μ_F be a probability measure on Ω_F; then μ_F is a random field on finite set F.

Let the interaction V be a real-valued, translationally invariant function on the disjoint union $\bigcup_{F \in \mathscr{F}} \Omega_F$. Let $F^c = Z^\nu \backslash F$. For every $F \in \mathscr{F}$, the conditional energy is defined as

$$U_F(x, y) = \sum_{F' \subseteq F} V(x|_{F'}) + \sum_{F' \in \mathscr{F}, F' \cap F \neq 0, F' \cap F^c \neq 0} V([x \vee y]|_{F'}) \quad \text{(A.1)}$$

where $x \in \Omega_F$ and $y \in \Omega_{F^c}$. Here $x|_{F'}$ indicates the restriction of x on F' and $x \vee y = z \in \Omega$ is the configuration with $z|_F = x$ and $z|_{F^c} = y$. The first term is the energy of $x \in \Omega_F$ on F and the second term is the interaction energy of x with "boundary condition" $y \in \Omega_F{}^c$. If the conditional energy exists, it defines a conditional probability measure on F,

$$\mu_F(x, y) = Z_F^{-1}(y) e^{-U_F(x, y)} \quad \text{(A.2)}$$

where

$$Z_F(y) = \sum_{x \in \Omega_F} e^{-U_F(x, y)} \quad \text{(A.3)}$$

Then $\mu_F(\bullet, y)$ is a Gibbs random field on $\mathscr{F}$.

Let $\{F_n\}_{n=0}^{\infty}$ be an increasing sequence of finite subsets of Z^ν. The $\lim_{n \to \infty} \mu_{F_n}(y|_{F_n^c}) = \mu$ is the thermodynamic limit of the Gibbs random field with interaction V and boundary condition y. The thermodynamic limit is called a Gibbs state; it is not necessarily unique; for example, the limit may depend on the particular sequence $\{F_n\}$ or the boundary condition.

In general, a sufficient condition for the convergence of the conditional energy is that the interaction density is finite.[1] Consequences of μ being a Gibbs state include:

1. The conditional probability $\mu_F(\bullet, y)$ on finite subset F is continuous w.r.t. $y \in \Omega^{F^c}$ for all $F \in \mathscr{F}$.

2. Let g be a continuous function on Ω. Let $\langle g \rangle_F(z|_{F^c})$ be the expectation value of g on F with boundary condition $z|_{F^c}$,

$$\langle g \rangle_F(z|_{F^c}) = \sum_{x \in \Omega_F} g(x \vee z|_{F^c})\, \mu_F(x, z|_{F^c}) \tag{A.4}$$

where $z \in \Omega$. Then

$$\int_\Omega g(z)\, d\mu(z) = \int_\Omega \langle g \rangle_F(z|_{F^c})\, d\mu(z) \tag{A.5}$$

for all $F \in \mathscr{F}$ and continuous functions g on Ω. These are known as the DLR (Dobrushin–Lanford–Ruelle) equations.[1-3]

3. μ minimizes the free energy $F/T = \langle U \rangle - S$, where S is the entropy for fixed $\langle U \rangle$.

Note that 1 and 2 are sufficient conditions for μ to be a Gibbs state.

APPENDIX B

In this Appendix we obtain the probabililties needed to generate μ_1. As in Section 4, let $t = 0$ for the initial configuration and let the initial distribution μ_0 on $\Omega_0 = \{0, 1, M\}^Z$ be the uniform product distribution which assigns probability 1/3 to each cell state. Using the T_1 subphase rules (Table I), we find

$$\begin{aligned} &\text{if} \quad a_{i,1} = M, \quad \text{then } a_{i,0} = 0 \\ &\text{if} \quad a_{i,1}a_{i+1,1} = 01, \quad \text{then } a_{i,0} = 0 \\ &\text{if} \quad a_{i-1,1}a_{i,1} = 10, \quad \text{then } a_{i,0} = 0 \\ &\text{if} \quad a_{i-1,1}a_{i,1}a_{i+1,1} = 000, \quad \text{then } a_{i,0} = 1 \end{aligned} \tag{B.1}$$

Therefore, if the sequence $a_1 a_2 \cdots a_{m-1}$ contains any of the subsequences M, 01, 10, or 000, no additional information about the state of cell 0 can be found from the state of cell m; the conditional probability is independent of a_m,

$$P_m(a_0 | a_1 \cdots a_{m-1} a_m) = P_{m-1}(a_0 | a_1 \cdots a_{m-1}) \tag{B.2}$$

Actually, $P_3(a|000) = P_2(a|00)$, so only $P_2(a|00)$ is needed. For $m \geqslant 2$ the only sequences not containing these subsequences are the sequences consisting of all 1's. A sequence of 1's must end with 0, so we also need the conditional probabilities of the form $P_m(a|11\cdots110)$.

The μ_1 probability of small length $0M1$ sequences $a_1 a_2 \cdots a_{m-1} a_m$ can be easily found; just apply the local CA rules to the middle m cells of all configurations in $\mathscr{A}^{m+2}$, count the number of times the sequence $a_1 \cdots a_m$ appears, and divide by $|\mathscr{A}|^{m+2}$. The conditional probability is then simply

$$P_m(a \mid a_1 \cdots a_m) = P_{m+1}(a a_1 \cdots a_m)/P_m(a_1 \cdots a_m)$$

This method is impractical for finding $P_m(011 \cdots 110)$ for large m. Using the T_1 subphase rules (Table I), we find that if $a_{m,1} = 1$, $a_{m,0}$ may be either 1 or M and

$$\begin{aligned} &\text{if} \quad a_{m,1} = 1 \text{ and } a_{m,0} = 1, \quad \text{then,} \\ &\quad \text{with prob 1,} \quad a_{m+1,0} = M \text{ and } a_{m+1,1} = 1 \end{aligned}$$

and

$$\text{if} \quad a_{m,1} = 1 \text{ and } a_{m,0} = M, \quad \text{then} \begin{cases} \text{with prob. } \frac{1}{9}, & a_{m+1,0} = 1 \text{ and } a_{m+1,1} = 1 \\ \text{with prob. } \frac{1}{3}, & a_{m+1,0} = M \text{ and } a_{m+1,1} = 1 \\ \text{with prob. } \frac{5}{9}, & a_{m+1,1} = 0 \end{cases} \tag{B.3}$$

Then

$$P_m(01 \cdots 10) = P_m(01 \cdots 10 \text{ and } a_{m,0} = 1) + P_m(01 \cdots 10 \text{ and } a_{m,0} = M) \tag{B.4}$$

and

$$P_m(011 \cdots 10) = \tfrac{5}{9} P_{m-1}(01 \cdots 10 \text{ and } a_{m-1,0} = M) \tag{B.5}$$

(B.3) is a recursion relation for the probabilities $P_m(01 \cdots 10 \text{ and } a_{m,0} = 1)$ and $P_m(01 \cdots 10 \text{ and } a_{m,0} = M)$,

$$\mathbf{P}_m = \begin{vmatrix} P_m(01 \cdots 10 \text{ and } a_{m,0} = 1) \\ P_m(01 \cdots 10 \text{ and } a_{m,00} = M) \end{vmatrix} = \begin{bmatrix} 0 & 1/9 \\ 1 & 1/3 \end{bmatrix} \mathbf{P}_{m-1} \tag{B.6}$$

The eigenvalues of the transfer matrix are $\frac{1}{6}(1 \pm \sqrt{5})$. Asymptotically only the eigenvector with the larger eigenvalue is significant, so for large m, $\mathbf{P}m = \frac{1}{6}(1 + \sqrt{5})\,\mathbf{P}_{m-1}$. The initial vector $\mathbf{P}_2$ can be obtained from the probability of length-2 $0M1$ sequences: $P_2(10 \text{ and } a_{2,0} = 1) = 1/27$ and $P_2(10 \text{ and } a_{2,0} = M) = 5/27$. Then $P_m(011 \cdots 10)$ and $P_m(11 \cdots 10)$ are easily obtained by applying the relations (B.4)–(B.6) to $\mathbf{P}_2$.

ACKNOWLEDGMENTS

The author is grateful to Y. Oono for many useful discussions and comments and for critical reading of the manuscript. This work is supported in part by NSF grant DMR-86-12860 through the University of Illinois Materials Research Laboratory, and by DMR-87-01393.

REFERENCES

1. D. Ruelle, *Statistical Mechanics* (Duke University, Durham, North Carolina, 1975); *Thermodynamic Formalism* (Benjamin, New York, 1978).
2. R. L. Dobrushin, *Theory Prob. Appl.* **13**:197 (1968).
3. O. E. Lanford, in *Lecture Note in Physics*, Vol. 20, A. Lenard, ed. (Springer, Berlin, 1973).
4. Y. Oono and M. Kohmoto, *Phys. Rev. Lett.* **55**:2927 (1985).
5. Y. Takahashi, private communication (1985).
6. Y. Oono and C. Yeung, *J. Stat. Phys.* **48**:593 (1987).
7. Y. Kuramoto and T. Yamada, *Prog. Theor. Phys.* **56**:679 (1976); T. Yamada and Y. Kuramoto, *Prog. Theor. Phys.* **56**:681 (1976); Y. Kuramoto, *Prog. Theor. Phys. Suppl.* **64**:346 (1978); H. Yamazaki, Y. Oono, and K. Hirakawa, *J. Phys. Soc. Jpn.* **44**:335 (1978); **46**:721 (1979).
8. T. Winfree, *Sci. Am.* **230**:82 (1978); J. J. Tyson, in *The Belousov–Zhabotinsky Reaction*, S. Levine, ed. (Springer, Berlin, 1976).
9. J. Demongeot, E. Cole, and M. Tchuente, *Dynamical Systems and Cellular Automata* (Academic Press, New York, 1985).
10. S. Wolfram, *Theory and Applications of Cellular Automata* (World Scientific, Singapore, 1986).
11. Ya. Sinai, *Sov. Math. Dokl.* **4**:1818 (1963).
12. M. Aizenmann, S. Goldstein, and J. L. Lebowitz, *Commun. Math. Phys.* **39**:289 (1975).
13. P. Walters, *An Introduction to Ergodic Theory* (Springer, New York, 1982).
14. H. van Beijeren and L. S. Schulman, *Phys. Rev. Lett.* **53**:806 (1984).
15. J. Krug, J. L. Lebowitz, H. Spohn, and M. Q. Zhang, *J. Stat. Phys.* **44**:535 (1986).
16. A. DeMasi, P. A. Ferrari, and J. L. Lebowitz, *Phys. Rev. Lett.* **55**:1947 (1985); A. DeMasi, P. A. Ferrari, and J. L. Lebowitz, *J. Stat. Phys.* **44**:589 (1986); J. M., Gonzalez-Miranda, P. L. Garido, J. Marro, and J. L. Lebowitz, *Phys. Rev. Lett.* **59**:1934 (1987).
17. R. Dickman, *Phys. Lett. A* **122**:463 (1987).